General relativistic turbulence in spherically symmetric core-collapse supernovae simulations

L. Boccioli* and G. J. Mathews

Center for Astrophysics, Department of Physics, University of Notre Dame, 225 Nieuwland Science Hall, Notre Dame, IN 46556, USA
**E-mail: lbocciol@nd.edu*

E. P. O'Connor

The Oskar Klein Centre, Department of Astronomy, Stockholm University, AlbaNova, SE-106 91 Stockholm, Sweden

It is generally believed that General Relativity (GR) is of secondary importance in the explosion of core-collapse supernovae (CCSN). However, as 3D simulations are becoming more and more detailed, GR effects can be strong enough to change the hydrodynamics of the supernova and affect the explosion. Since a 3D simulation in full GR is computationally extremely challenging, it is valuable to modify simulations in a spherically symmetric spacetime to incorporate 3D effects. This permits exploration of the parameter dependence of CCSN with a minimum of computational resources. In this proceedings contribution we report on the formulation and implementation of general relativistic neutrino-driven turbulent convection in the spherically symmetric code `GR1D`. This is based upon *STIR*, a recently proposed Newtonian model based on mixing length theory. When the parameters of this model are calibrated to 3D simulations, we find that our GR formulation significantly alters the correspondence between progenitor mass and explosion vs. black-hole formation. We therefore believe that, going forward, simulating CCSNe in full GR is of primary importance.

Keywords: Supernovae - Simulations - Mixing Length Theory - General Relativistic Hydrodynamics

1. Introduction

This proceedings contribution is based on work published in Ref. [1]. Core-collapse supernovae (CCSNe) have been at the core of cutting-edge computational research for more than 50 years. Despite that, the details of the mechanisms driving the explosion still remain unknown, even though significant progress has been made since the first attempts at explaining CCSNe.[2–4]

Historically, one-dimensional (1D) spherically symmetric simulations were able to assess the crucial role of neutrinos in aiding the expansion of the shock through the so-called delayed neutrino-heating mechanism.[5,6] Two-dimensional (2D) simulations[7,8] and three-dimensional (3D) simulations,[9] have been only recently accessible thanks to the fast technological improvements of the last three decades.

Spherically symmetric simulations, however, have unfortunately, not led to self-consistent explosions of Fe-core CCSNe (which are the most common) since they involve all stars with masses > 11 $M_\odot$. On the other hand, there have been several simulations in 2D and 3D that have led to successful explosions.[10–16] However, 2D simulations have been recently shown[17] to favor explosions by an artificial enhancement of neutrino-heating behind the shock via an inverse turbulence cascade which is not present in 3D. Therefore, only 3D simulations can provide the final explanation as to what causes the explosion. However, despite the technological improvements of the last few decades, 3D simulations continue to present a difficult computational challenge, even for modern supercomputers.

In comparison, modern 1D simulations are significantly faster to run and are also more consistent across different codes.[18] In other words, when the initial conditions are the same, different groups obtain similar results. This guarantees a somewhat solid foundation, making 1D simulations an ideal tool to study how different input physics can affect the explosion of supernovae. To do that, first one needs to artificially trigger an explosion. In a recent paper Couch et al.[19] (hereafter CWO20) developed *STIR* (Simulated Turbulence In Reduced-dimensionality), a parametric model based upon Mixing Length Theory (MLT) that incorporates the effects of 3D turbulence in spherically symmetric simulations.

The simulations from CWO20 use Newtonian hydrodynamics and only partially include general relativistic effects through a General Relativistic Effective Potential (GREP) from Ref. [20], which is a common practice in the supernova community. However, we know that General Relativity (GR) plays an important role in the explosion of supernovae.[10,21] Hence, simulations in full GR are desirable, and in this proceedings contribution we summarize the extension of the *STIR* model to a general relativistic treatment.[1] Throughout the manuscript, we adopt natural units, i.e. $G = c = M_\odot = 1$.

2. Methods

2.1. *The STIR model of Couch et al. (2020)*

A detailed description of STIR can be found in Refs. 22, 23 and CWO20. There, it is shown that the effects of turbulence can be treated as a perturbation on the background fluid. After a Reynolds decomposition of the compressible Euler equations, and several other approximations valid in typical supernova thermodynamic environments, one arrives to the following equation describing the evolution of the turbulent kinetic energy:

$$\begin{aligned}\frac{\partial \rho v_{\rm turb}^2}{\partial t} + \frac{1}{r^2}\frac{\partial}{\partial r}[r^2(\rho v_{\rm turb}^2 v_r - \rho D_K \nabla v_{\rm turb}^2)] \\ = -\rho v_{\rm turb}^2 \frac{\partial v_r}{\partial r} + \rho v_{\rm turb}\omega_{\rm BV}^2 \Lambda_{\rm mix} - \rho \frac{v_{\rm turb}^3}{\Lambda_{\rm mix}} \quad ,\end{aligned} \tag{1}$$

where

$$\Lambda_{\rm mix} = \alpha_{\rm MLT} \frac{P}{\rho g}, \tag{2}$$

$$\omega_{\rm BV}^2 = g_{\rm eff} \left(\frac{1}{\rho} \frac{\partial \rho}{\partial r} - \frac{1}{\rho c_s^2} \frac{\partial P}{\partial r} \right). \tag{3}$$

In the above equations, ρ is the mass density, v_r is the radial velocity, $\Lambda_{\rm mix}$ is the mixing length, $\omega_{\rm BV}$ is the Brunt-Väisälä frequency, c_s is the sound speed, D_K is a diffusion coefficient due to turbulence and $g_{\rm eff}$ is the magnitude of the local effective acceleration. For a fluid in hydrostatic equilibrium, $g_{\rm eff}$ simply reduces to the local gravitational acceleration g. More generally, however, in the rest frame one should take the acceleration of the fluid into account. Therefore, the total acceleration $g_{\rm eff}$ can be expressed as:

$$g_{\rm eff} = g - v_r \frac{\partial v_r}{\partial r} \ , \tag{4}$$

as described in CWO20.

The mixing length $\Lambda_{\rm mix}$ is the average distance that a convective element will travel before being mixed with (and increasing the internal energy of) the surrounding material. The Brunt-Väisälä frequency $\omega_{\rm BV}$ is the rate at which the convective elements are rising. As one can notice from Eq. (3), $\omega_{\rm BV}^2$ can be either positive or negative: when $\omega_{\rm BV}^2 > 0$ the fluid is convectively unstable, i.e. convection is generated; when $\omega_{\rm BV}^2 < 0$ the fluid is convectively stable, i.e. convection is damped. Ultimately, the main parameter of the model is $\alpha_{\rm MLT}$, which scales the mixing length to the pressure scale height in Eq. (2). Typically $\alpha_{\rm MLT} \sim O(1)$.

The diffusion coefficient D_K is defined as:

$$D_K = \alpha_K v_{\rm turb} \Lambda_{\rm mix} \ . \tag{5}$$

Similar terms appear in the internal energy, electron fraction, and neutrino energy density evolution equations (for the complete set of hydrodynamic equations used in the model, (see Eqs. 25-29 and 33 in CWO20). Therefore, strictly speaking, *STIR* has 4 additional free parameters: α_K, α_e, $\alpha_{\rm Ye}$, α_ν. However, the convective motions are not very sensitive to the value of these parameters, so we set them to 1/6 for simplicity, consistent with the choices of Ref. [24] and CWO20.

In the next section we describe a general relativistic version of the model described above.

2.2. *STIR in General relativity*

The first attempts to create a general relativistic model for convection date back to Ref. [25]. We follow the same approach, but using a slightly different formalism.

All the simulations described here[1] were run with the open-source, spherically symmetric, general relativistic code `GR1D`.[26] The Boltzmann equation for neutrino

transport is solved using an M1-scheme, with opacity tables generated using the open-source code `NuLib`.[27]

The metric evolved in `GR1D` is Schwarzchild-like:

$$\begin{aligned} ds^2 &= g_{\mu\nu} x^\mu x^\nu \\ &= -\alpha(r,t)^2 dt^2 + X(r,t)^2 dr^2 + r^2 d\Omega^2, \end{aligned} \tag{6}$$

where α and X can be expressed as functions of a metric potential ϕ (which reduces to the Newtonian potential in the Newtonian limit) and the enclosed gravitational mass $M_{\rm grav}$:

$$\begin{aligned} \alpha(r,t) &= \exp[\phi(r,t)], \\ X(r,t) &= \left(1 - \frac{2M_{\rm grav}(r,t)}{r}\right)^{-1/2}. \end{aligned} \tag{7}$$

For the present work, we first note that turbulence is mostly relevant far from the proto-neutron star (PNS) where GR effects can be treated as a perturbation. Therefore, one can simply make a few changes to the terms in Eq. (1) without having to re-derive the entire Reynold's decomposition. The expression for $\omega^2_{\rm BV}$, however, must be carefully re-derived. Far from the PNS, we invoke the following:

(1) replace the conserved variable ρ with its GR counterpart, i.e. $D = WX\rho$, where $W = (1-v^2)^{-1/2}$ and $v = Xv_r$;
(2) multiply the RHS of Eq. (1) by αX.
(3) multiply the spatial flux in Eq. (1) by α/X (see Ref. [26] for more details on the derivation of the hydrodynamic equations in `GR1D`).

The expression of $\omega^2_{\rm BV}$ can be derived using conservation of momentum for a convective eddy in a background fluid in hydrostatic equilibrium. The case of a fluid with non zero acceleration can be derived with ad-hoc corrections for general relativistic effects. The derivation can be found in Ref. [1], and it leads to:

$$\omega^2_{\rm BV} = \frac{\alpha^2}{\rho h X^2}\left(\frac{{\rm d}\phi}{{\rm d}r} - v\frac{\partial v}{\partial r}\right)\left(\frac{\partial \rho(1+\epsilon)}{\partial r} - \frac{1}{c_s^2}\frac{\partial P}{\partial r}\right), \tag{8}$$

where $v = Xv_r$.

The main difference between Eqs. (3) and (8) is the inclusion of $\partial\rho\epsilon/\partial r$ in the latter. In the gain region the internal energy decreases with radius, i.e. $\partial\rho\epsilon/\partial r < 0$. This decreases the magnitude of $\omega_{\rm BV}$ and therefore the amount of turbulence that is generated. We will come back to this in Section 3.2

3. Results: Comparison with 3D simulations

3.1. *Results using an effective potential*

Inspired by the work of CWO20, we compare our GREP model to the `mesa20_LR_v` 3D simulation,[28] by using the same setup chosen by CWO20. That is, we simulate

the collapse of a 20 $M_\odot$ progenitor from,[29] adopting the SFHo EOS[30] and assuming Nuclear Statistical Equilibrium (NSE) everywhere. The algorithm used in `FLASH` to solve the neutrino radiation transport closely resembles the one used in `GR1D`.[27] Additionally, the set of `NuLib` opacities we adopted is the same used by CWO20. Finally, we use 12 neutrino energy groups geometrically spaced up to ∼250 MeV.

The upper panels of Figure 1 (modified from Ref. [1]) show the shock radius versus time and the turbulent velocity profile at ∼135 ms post-bounce for our GREP model (to be compared to Figures 1 and 2 of CWO20). The main difference between our results using `GR1D` and the ones from CWO20 using `FLLASH` is that `GR1D` consistently gives larger values for the turbulent velocity at a given $\alpha_{\rm MLT}$. This then translates into larger shock radii at a given time. Except for these small differences, the agreement between the two models is very good, and both yield explosions for $\alpha_{\rm MLT} \gtrsim 1.2$.

When it comes to the comparison with the 3D results, however, our MLT-like model does not captures some features that are present in the 3D case. Specifically, the profile at ∼135 ms post-bounce of the convective speed in 3D has a longer tail at 50-80 km. This has already been noticed by CWO20, and it is due to angular variations present in the 3D model, rather than a deeper convection extending in the region below the gain layer. In our model, convection shuts off at 80 km, as one would expect, since that is approximately the location of the gain layer. A more interesting difference is the lack of PNS convection at 25 km, not captured by our MLT-like model. A possible explanation for this is that STIR is not taking lepton number-driven convection into account, which is not easily tractable with MLT models, and therefore a more careful treatment of this type of convection might ease the discrepancy with the 3D results. We are currently working on adjusting some of the parameters of STIR deep inside the PNS to match the 3D result, and therefore analyze the impact of PNS convection on the explosion, but this goes beyond the scope of this conference proceedings.

3.2. *Results using GR*

One can compare the results obtained using the simple GREP approach with results in full GR. We show the results using full GR in the bottom panels of Figure 1, while the upper panels refer to the runs using our GREP model. The most important difference to point out is the range of $\alpha_{\rm MLT}$ used in the GR and GREP simulations. To produce shock radii and turbulent velocities that are similar to the GREP results, the value of $\alpha_{\rm MLT}$ that needs to be used in full GR is $\sim$ 20% larger. The reason behind this increase in $\alpha_{\rm MLT}$ lies in the expression of $\omega_{\rm BV}$. As pointed out in Section 2.2, including the internal energy gradient into eq. (8) is the main difference between the GREP and GR models.

In the gain region, where turbulent convection is most relevant, the gradient of the internal energy is negative. This decreases the magnitude of $\omega^2_{\rm BV}$, making the fluid more stable against convection. Including $\rho\epsilon$ in the definition of $\omega_{\rm BV}$ is hence

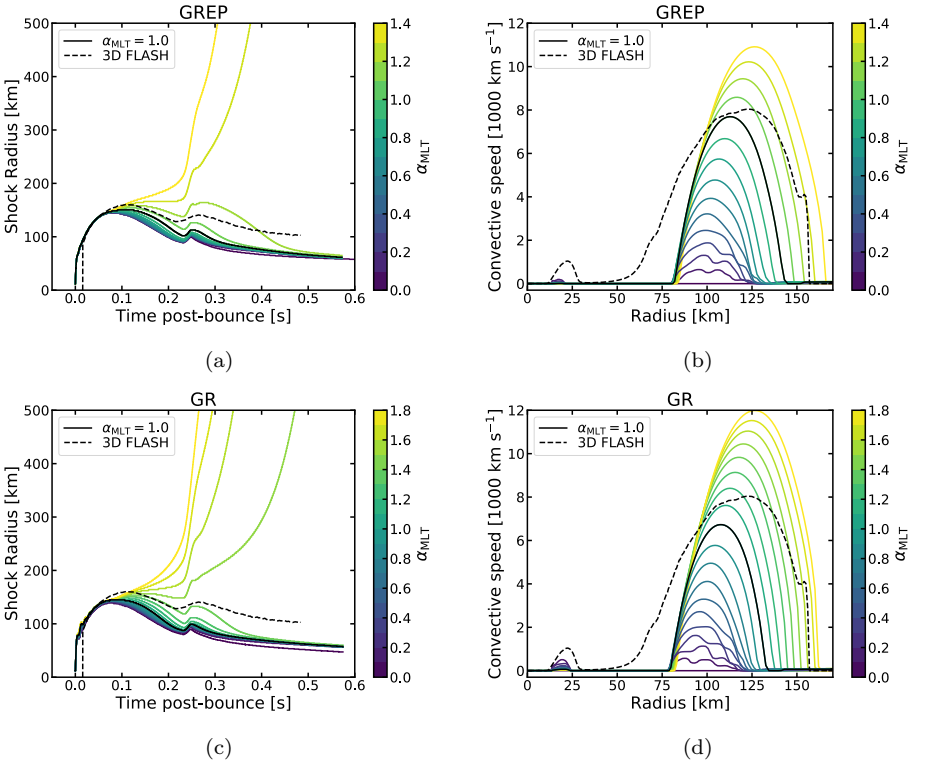

Fig. 1. The plots on the upper row were generated using our GREP model, while the plots on the bottom row were generated using full GR. Panels (a,c) show the time evolution of the shock radius for different values of the parameter $\alpha_{\rm MLT}$, and can be compared to Figure 2 from CWO20. Panels (b,d) show a snapshot at ~ 135 ms post bounce of $v_{\rm turb}$, and can be compared to Figure 1 from CWO20. The dashed lines represent the 3D simulation from Ref. [28].

needed to realistically characterize turbulent convection. If one takes the form of $\omega_{\rm BV}$ from Eq. (8) and implements it in the GREP model, the value of $\alpha_{\rm MLT}$ needed to achieve an explosion increases, becoming comparable to the one used in the GR model.

3.3. *Progenitor Study*

In the previous Sections we summarized the validation of our turbulent convection model[1] by comparing it to the 3D results of Ref. [31]. In this section, we summarize the use[1] of our calibrated models to simulate the collapse and subsequent shock revival of 20 progenitors from Ref. [32]. We use three different values of $\alpha_{\rm MLT}$, for which the fraction of successful explosions is roughly between 25% and 80%.

Our GREP model generates results[1] that are compatible with the ones obtained by CWO20 shifted by $\Delta\alpha_{\rm MLT} \simeq 0.05$. If one compares the left panel of Figure 2 with Figure 6 from CWO20, it is clear that our model tends to yield explosions for

slightly smaller values of $\alpha_{\rm MLT}$. This shift mainly depends on two differences between our model and the one from CWO20: (i) we used a finer resolution in space and energy; (ii) the numerical algorithms used to solve the hydrodynamic equations and the neutrino transport are different.

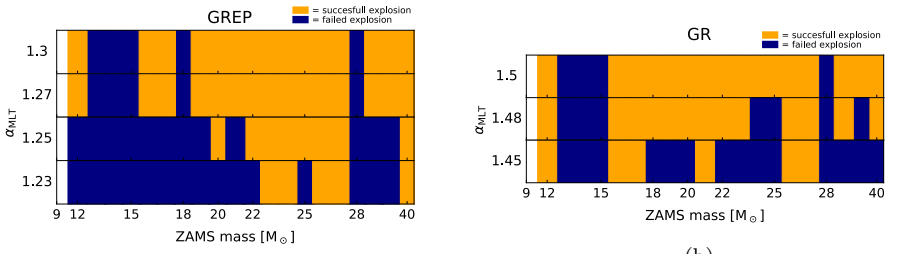

Fig. 2. Explosion pattern (modified from Ref. [1]) of CCSN for the GREP (left panel) and GR (right panel) models as a function of the Zero Age Main Sequence mass. Orange bands represent successful explosions (i.e. the shock has reached 500 km), while dark blue bands represent failed explosions.

Even more importantly, Figure 2 shows that a General Relativistic treatment of turbulent convection does not simply reproduce the results obtained by the GREP model. By looking at Figure 1 one might conclude that, since the value of $\alpha_{\rm MLT}$ required to generate an explosion in GR is larger, using GR with larger values of $\alpha_{\rm MLT}$ would produce the same patterns shown in the left panel of Fig. 2. However, that is not the case, and GR modifies the explosion pattern of CCSNe. To even more accurately characterize the differences between the patterns of explodability in the GR and GREP models, a systematic study with hundreds of progenitors and more values of $\alpha_{\rm MLT}$ would be desired. That, however, is beyond the scope of this conference proceedings.

We can conclude from Figure 2 that general relativity changes which progenitors are more likely to explode. By focusing on the patterns associated with $\alpha_{\rm MLT} = 1.27$ and $\alpha_{\rm MLT} = 1.48$ one can see that, using the GREP model, the 24, 25 and 30 $M_\odot$ progenitors explode, whereas the 18 $M_\odot$ doesn't. In the GR model it is the exact opposite. It should be pointed out that the pattern of explodability generated by the GR model with $\alpha_{\rm MLT} = 1.48$ is intermediate between the results of CWO20 and Ref. [32]: (i) like the former (but unlike the latter), it shows failed explosions for low mass progenitors with M = 13-15 $M_\odot$; (ii) like the latter (and unlike the former) it shows that higher mass progenitors with M = 24-25 $M_\odot$ result in failed explosions.

It is worth mentioning that the explodability pattern obtained using the GR model with $\alpha_{\rm MLT} = 1.48$ cannot be reproduced by the GREP model. One can see that, from the left panel of Figure 2, for $\alpha_{\rm MLT} = 1.23$, the 25 $M_\odot$ progenitor fails, and all progenitors below 22 $M_\odot$ fail as well. This shows that the GREP model

cannot produce successful explosions for progenitors with masses 15-18 $M_\odot$ and at the same time failed explosions of the 24-25 $M_\odot$ progenitors, like we see in the right panel of Figure 2. Notably, the GR model with $\alpha_{\rm MLT} = 1.5$ reproduces the same pattern of explodability found in the GREP model with $\alpha_{\rm MLT} = 1.27$ (with the only exception of the 18 $M_\odot$ progenitor). This tells us that: (i) the threshold between failed and successful explosions is a steep function of $\alpha_{\rm MLT}$; and (ii) GR can reproduce the GREP results for large values of $\alpha_{\rm MLT}$ and large explosion fractions.

Overall, our results[1] have shown that including general relativistic effects can modify how turbulence behaves in a one-dimensional, MLT-like model. It is hard to predict if this effect will translate to multi-dimensional simulations, given the differences between 1D and multi-D. Nonetheless, these results suggest that GR (as opposed to GREP) can have a significant impact on the explosion of CCSNe. A detailed comparison between full-GR and Newtonian simulations, performed with 2D and 3D codes across multiple progenitors, will clarify whether this effect translates to higher dimensions, where turbulent convection is generated self-consistently.

4. Conclusions

In this proceedings contribution we have summarized our development[1] of extended *STIR*, the MLT-like model of CWO20, to a full general relativistic formalism. Our implementation of STIR in `GR1D` can reproduce the results of CWO20 when using the same GREP model that they developed. The GR version of STIR needs larger values of $\alpha_{\rm MLT}$ to achieve shock dynamics that are similar to the ones obtained with a GREP model.[1] The reason behind this is that, as can be seen from Eq. (8), one needs to include the gradient of the internal energy gradient in the expression for $\omega_{\rm BV}$. This reduces the magnitude of $\omega^2_{\rm BV}$ in the gain region, which inhibits the generation of turbulence. The net result is that larger values of $\Lambda_{\rm mix}$ (and therefore of $\alpha_{\rm MLT}$) are needed to develop a convective mixing that is as strong as the one obtained without the inclusion of GR.

After comparing our model to the 3D results of Ref. [28], we simulated[1] the collapse and subsequent shock expansion of 20 different progenitors[32] for different values of $\alpha_{\rm MLT}$, for both the GREP and GR models. Our main finding[1] is that GR changes the pattern of explodability of CCSNe. Specifically, the 24 $M_\odot$ and the 25 $M_\odot$ progenitors need comparatively much larger values of $\alpha_{\rm MLT}$ to explode with the GR model. This produces an explodability as a function of progenitor mass that is intermediate between the results of CWO20 and Ref. [32]. However, the GR model also shows, for values of $\alpha_{\rm MLT}$ that yield large explosion fractions (i.e. $\alpha_{\rm MLT} = 1.5$), an explodability that is compatible with the results obtained using the GREP model.

Acknowledgments

The authors would like to thank Sean Couch, Andre da Silva Schneider and Mackenzie Warren for fruitful discussions. Work at the University of Notre Dame supported

by the U.S. Department of Energy under Nuclear Theory Grant DE-FG02-95-ER40934. EOC would like to acknowledge Vetenskapsrådet (the Swedish Research Council) for supporting this work under award numbers 2018-04575 and 2020-00452.

References

1. L. Boccioli, G. J. Mathews and E. P. O'Connor, General Relativistic Neutrino-driven Turbulence in One-dimensional Core-collapse Supernovae, *ApJ* **912**, p. 29 (May 2021).
2. S. A. Colgate and R. H. White, The Hydrodynamic Behavior of Supernovae Explosions, *ApJ* **143**, p. 626 (March 1966).
3. W. D. Arnett, Gravitational collapse and weak interactions, *Canadian Journal of Physics* **44**, 2553 (January 1966).
4. G. Sonneborn, B. Altner and R. P. Kirshner, The Progenitor of SN 1987A: Spatially Resolved Ultraviolet Spectroscopy of the Supernova Field, *ApJ* **323**, p. L35 (December 1987).
5. H. A. Bethe and J. R. Wilson, Revival of a stalled supernova shock by neutrino heating, *ApJ* **295**, 14 (August 1985).
6. S. W. Bruenn, Stellar core collapse - Numerical model and infall epoch, *ApJS* **58**, 771 (August 1985).
7. D. S. Miller, J. R. Wilson and R. W. Mayle, Convection above the Neutrinosphere in Type II Supernovae, *ApJ* **415**, p. 278 (September 1993).
8. M. Herant, W. Benz, W. R. Hix, C. L. Fryer and S. A. Colgate, Inside the Supernova: A Powerful Convective Engine, *ApJ* **435**, p. 339 (November 1994).
9. C. L. Fryer and M. S. Warren, Modeling Core-Collapse Supernovae in Three Dimensions, *ApJL* **574**, L65 (July 2002).
10. B. Müller, H.-T. Janka and A. Marek, A New Multi-dimensional General Relativistic Neutrino Hydrodynamics Code for Core-collapse Supernovae. II. Relativistic Explosion Models of Core-collapse Supernovae, *ApJ* **756**, p. 84 (September 2012).
11. E. J. Lentz, S. W. Bruenn, W. R. Hix, A. Mezzacappa, O. E. B. Messer, E. Endeve, J. M. Blondin, J. A. Harris, P. Marronetti and K. N. Yakunin, Three-dimensional Core-collapse Supernova Simulated Using a 15 $M_{\odot}$ Progenitor, *ApJL* **807**, p. L31 (July 2015).
12. H.-T. Janka, T. Melson and A. Summa, Physics of Core-Collapse Supernovae in Three Dimensions: A Sneak Preview, *Annual Review of Nuclear and Particle Science* **66**, 341 (October 2016).
13. S. W. Bruenn, E. J. Lentz, W. R. Hix, A. Mezzacappa, J. A. Harris, O. E. B. Messer, E. Endeve, J. M. Blondin, M. A. Chertkow, E. J. Lingerfelt, P. Marronetti and K. N. Yakunin, The Development of Explosions in Axisymmetric Ab Initio Core-collapse Supernova Simulations of 12-25 M Stars, *ApJ* **818**, p. 123 (February 2016).
14. E. P. O'Connor and S. M. Couch, Two-dimensional Core-collapse Supernova Explosions Aided by General Relativity with Multidimensional Neutrino Transport, *ApJ* **854**, p. 63 (February 2018).
15. B. Müller, T. M. Tauris, A. Heger, P. Banerjee, Y.-Z. Qian, J. Powell, C. Chan, D. W. Gay and N. Langer, Three-dimensional simulations of neutrino-driven core-collapse supernovae from low-mass single and binary star progenitors, *MNRAS* **484**, 3307 (April 2019).
16. A. Burrows, D. Radice, D. Vartanyan, H. Nagakura, M. A. Skinner and J. C. Dolence, The overarching framework of core-collapse supernova explosions as revealed by 3D FORNAX simulations, *MNRAS* **491**, 2715 (January 2020).

17. S. M. Couch and C. D. Ott, The Role of Turbulence in Neutrino-driven Core-collapse Supernova Explosions, *ApJ* **799**, p. 5 (January 2015).
18. E. O'Connor, R. Bollig, A. Burrows, S. Couch, T. Fischer, H.-T. Janka, K. Kotake, E. J. Lentz, M. Liebendörfer, O. E. B. Messer, A. Mezzacappa, T. Takiwaki and D. Vartanyan, Global comparison of core-collapse supernova simulations in spherical symmetry, *Journal of Physics G: Nuclear and Particle Physics* **45**, p. 104001 (sep 2018).
19. S. M. Couch, M. L. Warren and E. P. O'Connor, Simulating turbulence-aided neutrino-driven core-collapse supernova explosions in one dimension, *The Astrophysical Journal* **890**, p. 127 (feb 2020).
20. A. Marek, H. Dimmelmeier, H. T. Janka, E. Müller and R. Buras, Exploring the relativistic regime with Newtonian hydrodynamics: An improved effective gravitational potential for supernova simulations, *A&A* **445**, 273 (January 2006).
21. J. R. Wilson and G. J. Mathews, *Relativistic Numerical Hydrodynamics* (Cambridge University Press, 2003).
22. Q. A. Mabanta and J. W. Murphy, How Turbulence Enables Core-collapse Supernova Explosions, *ApJ* **856**, p. 22 (March 2018).
23. Q. A. Mabanta, J. W. Murphy and J. C. Dolence, Convection-aided Explosions in One-dimensional Core-collapse Supernova Simulations. I. Technique and Validation, *ApJ* **887**, p. 43 (December 2019).
24. B. Müller, M. Viallet, A. Heger and H.-T. Janka, The Last Minutes of Oxygen Shell Burning in a Massive Star, *ApJ* **833**, p. 124 (December 2016).
25. K. S. Thorne, Validity in General Relativity of the Schwarzschild Criterion for Convection, *ApJ* **144**, p. 201 (April 1966).
26. E. O'Connor and C. D. Ott, A new open-source code for spherically symmetric stellar collapse to neutron stars and black holes, *Classical and Quantum Gravity* **27**, p. 114103 (June 2010).
27. E. O'Connor, An Open-source Neutrino Radiation Hydrodynamics Code for Core-collapse Supernovae, *ApJS* **219**, p. 24 (August 2015).
28. E. P. O'Connor and S. M. Couch, Exploring Fundamentally Three-dimensional Phenomena in High-fidelity Simulations of Core-collapse Supernovae, *ApJ* **865**, p. 81 (October 2018).
29. R. Farmer, C. E. Fields, I. Petermann, L. Dessart, M. Cantiello, B. Paxton and F. X. Timmes, On Variations of Pre-Supernova Model Properties, *The Astrophysical Journal Supplement Series* **227**, p. 22 (dec 2016).
30. A. W. Steiner, M. Hempel and T. Fischer, Core-collapse Supernova Equations of State Based on Neutron Star Observations, *ApJ* **774**, p. 17 (September 2013).
31. S. M. Couch and E. P. O'Connor, High-resolution Three-dimensional Simulations of Core-collapse Supernovae in Multiple Progenitors, *ApJ* **785**, p. 123 (April 2014).
32. T. Sukhbold, T. Ertl, S. E. Woosley, J. M. Brown and H.-T. Janka, Core-Collapse Supernovae from 9 to 120 Solar Masses Based on Neutrino-Powered Explosions, *The Astrophysical Journal* **821**, p. 38 (April 2016).